

Supporting Information

Injectable Biodegradable Polymeric Complex for Glucose-Responsive Insulin Delivery

Jinqiang Wang^{‡,¶,†,§}, Zejun Wang^{†,§}, Guojun Chen^{†,§,▽}, Yanfang Wang[‡], Tianyuan Ci^{†,§}, Hongjun Li^{‡,†,§},
Xiangsheng Liu^{§,||}, Daojia Zhou^{†,§}, Anna R. Kahkoska[‡], Zhuxian Zhou^{||}, Huan Meng^{§,||,[⊥]}, John B. Buse[‡],
Zhen Gu^{‡,¶,||,||,†,§,[⊥]*}

[‡]College of Pharmaceutical Sciences, Zhejiang University, Hangzhou 310058, China;

[¶]MOE Key Laboratory of Macromolecular Synthesis and Functionalization, Department of Polymer Science and Engineering, Zhejiang University, Hangzhou 310027, China

^{||}Department of General Surgery, Sir Run Run Shaw Hospital, School of Medicine, Zhejiang University, Hangzhou 310016, China;

^{||}Zhejiang Laboratory of Systems & Precision Medicine, Zhejiang University Medical Center, Hangzhou 311121, China.

[†]Department of Bioengineering, University of California, Los Angeles, CA 90095, USA;

[§]California NanoSystems Institute, University of California, Los Angeles, CA 90095, USA;

^{||}Division of NanoMedicine, Department of Medicine, David Geffen School of Medicine, Los Angeles, CA 90095, USA;

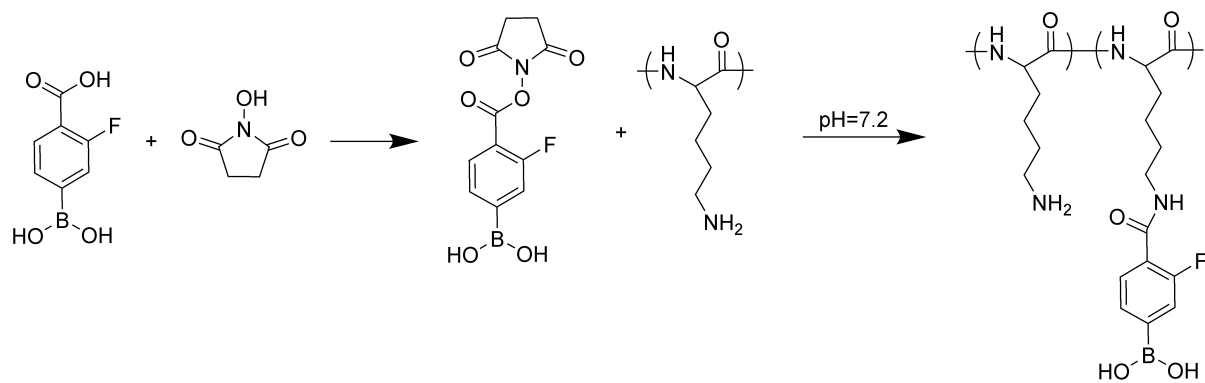
[‡]Department of Medicine, University of North Carolina School of Medicine, Chapel Hill, NC 27599, USA;

^{||}Key Laboratory of Biomass Chemical Engineering of Ministry of Education and Center for Bionanoengineering, College of Chemical and Biological Engineering, Zhejiang University, Hangzhou 310027, China;

[⊥]Jonsson Comprehensive Cancer Center, University of California, Los Angeles, CA 90024, USA;

[▽]Department of Biomedical Engineering, and the Rosalind & Morris Goodman Cancer Research Center, McGill University, Montreal, QC H3G 0B1, Canada

*E-mail: guzhen@zju.edu.cn



Scheme S1. Synthesis route of PLL-FPBA.

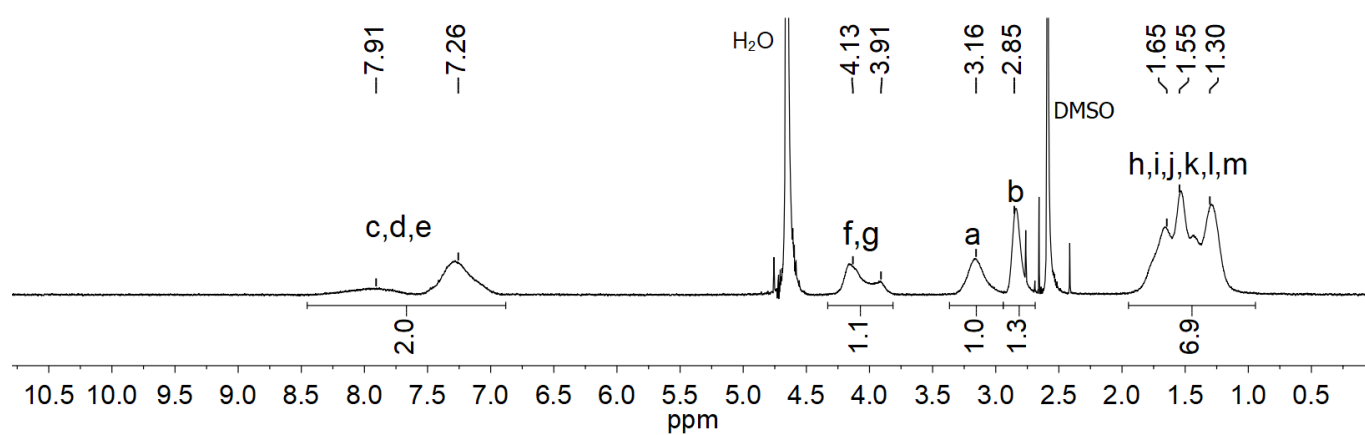
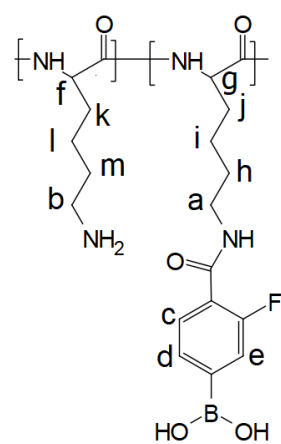


Figure S1. $^1\text{H-NMR}$ spectrum of FPBA modified PLL_{4-15k} in D₂O with TFA to adjust its pH. About 43% of the amino groups in this polymer was reacted with FPBA-NHS.

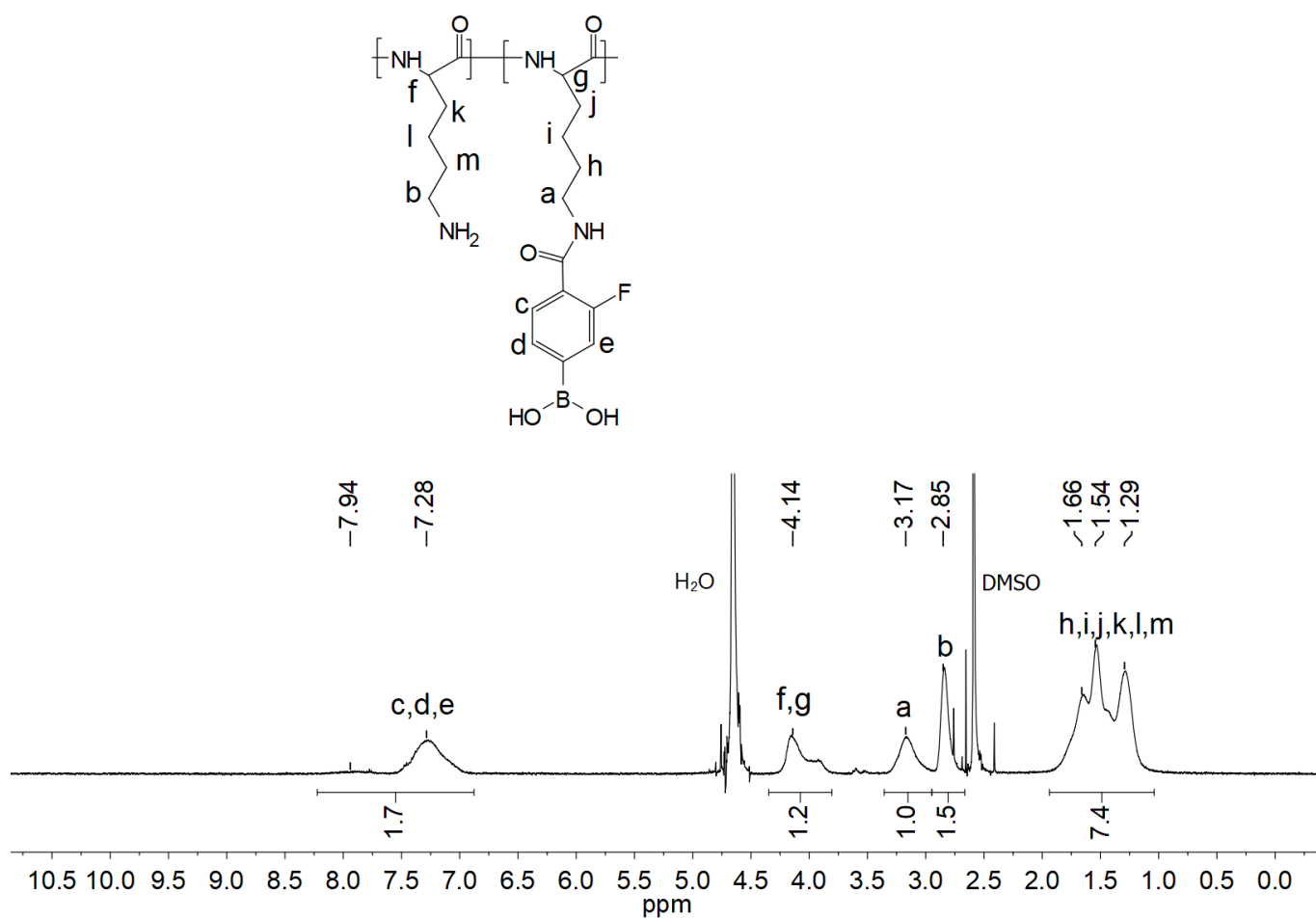


Figure S2. ¹H-NMR spectrum of FPBA modified PLL_{15-30k} in D₂O with TFA to adjust its pH. About 40% of the amino groups in this polymer was reacted with FPBA-NHS.

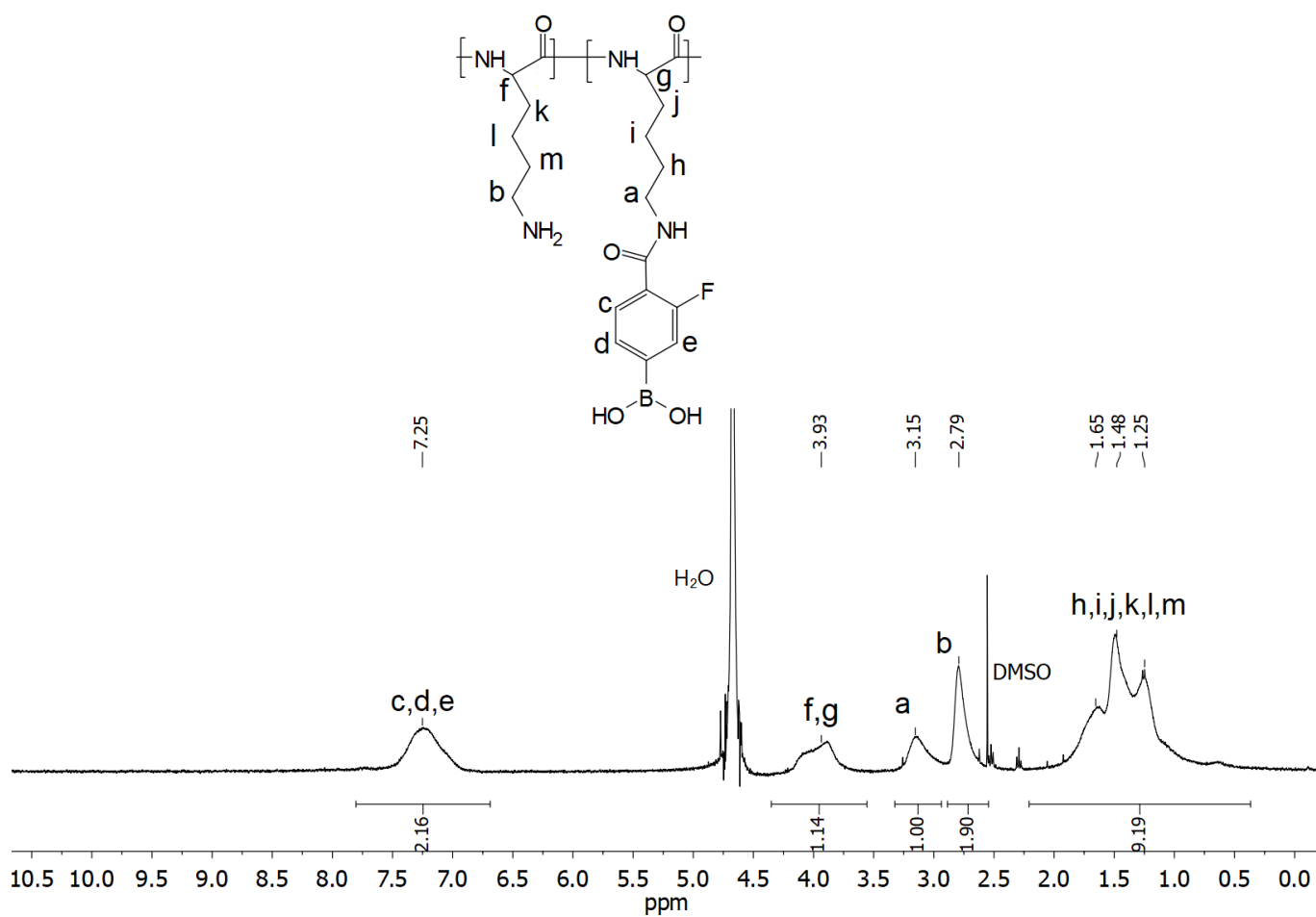


Figure S3. ¹H-NMR spectrum of FPBA modified PLL_{30k-70k} in D₂O with TFA to adjust its pH. About 35% of the amino groups in this polymer was reacted with FPBA-NHS.

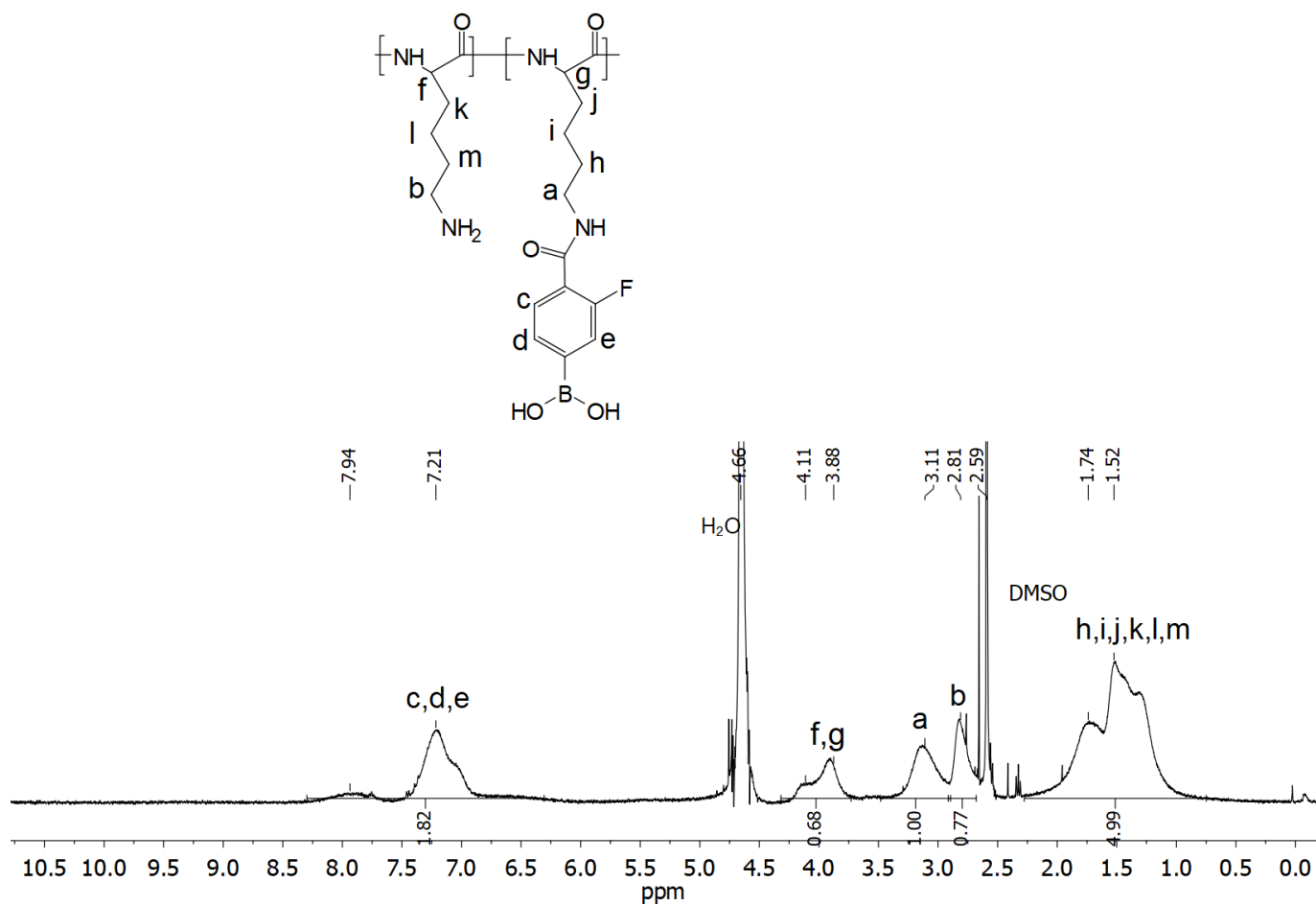


Figure S4. ¹H-NMR spectrum of FPBA modified PLL_{30-70k} in D₂O with TFA to adjust its pH. About 60% of the amino groups in this polymer was reacted with FPBA-NHS.

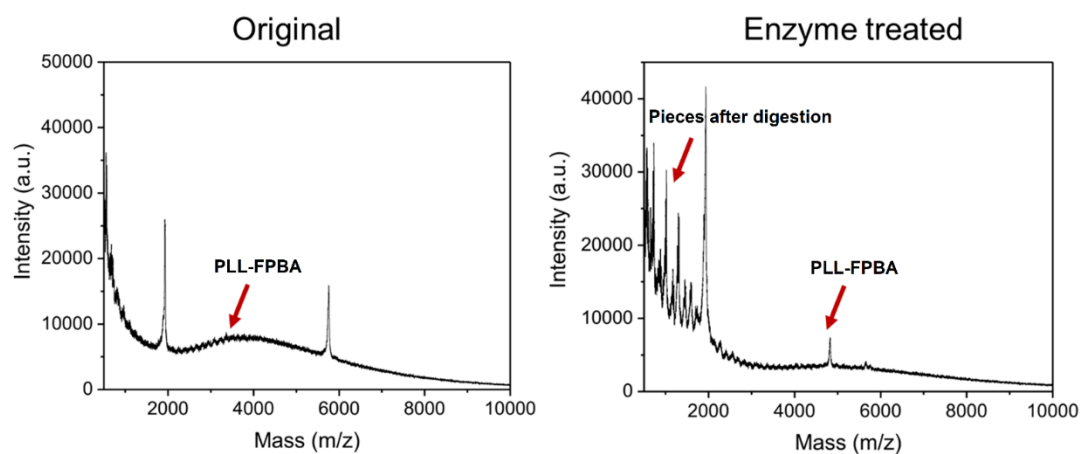


Figure S5. MALDI-TOF mass spectra of PLL_{0.4}-FPBA_{0.6} before and after enzyme digestion. The concentration of the polymer was 20 mg/mL, while the 0.1 mg/mL of trypsin was used. The polymer was incubated with trypsin at 37 °C overnight on a shaker (300 rpm).

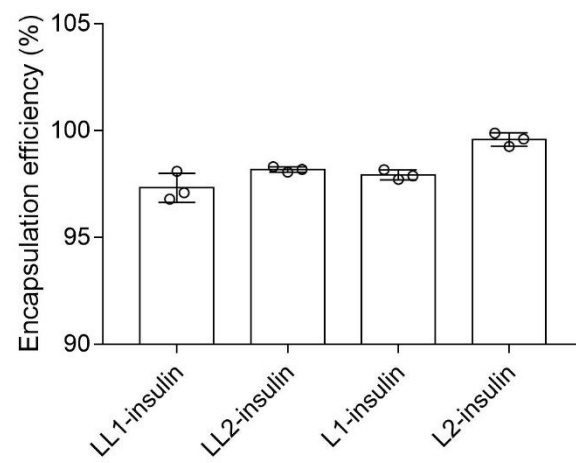


Figure S6. The encapsulation efficiency of insulin for various complexes. Data are mean \pm SD ($n=3$).

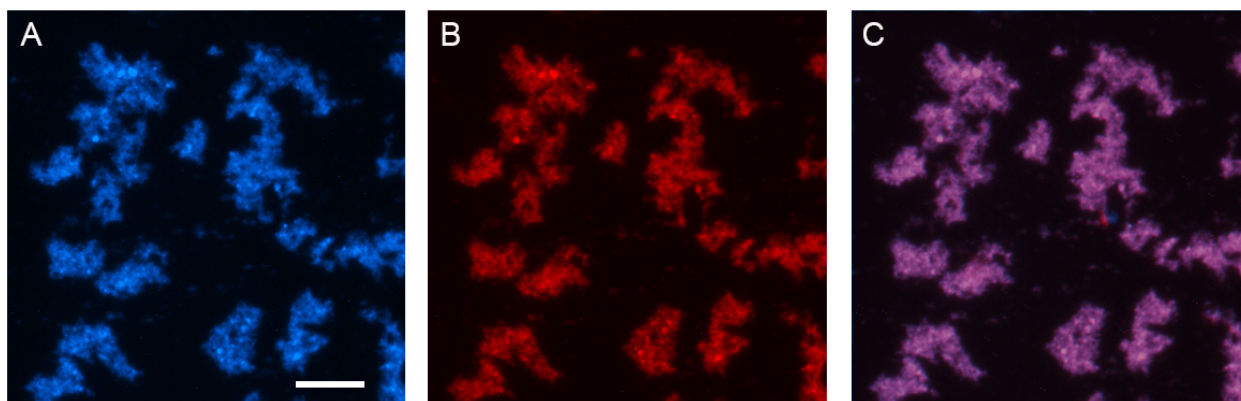


Figure S7. Fluorescence images of insulin complex. (A) Representative image of the complex observed from the channel of Cy5-labeled polymer. (B) Representative image of complex observed from the channel of Rhodamine B-labeled insulin. (C) Merge of images (A) and (B). Scale bar, 20 μm .

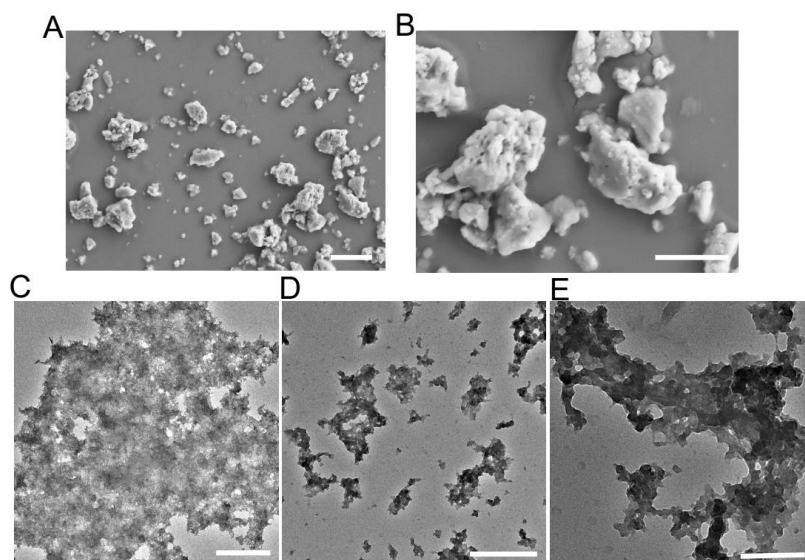


Figure S8. Representative SEM and TEM images of L2-insulin. (A-B) Representative SEM images of L2-insulin. Scale bars are 10 μm (A) and 5 μm (B), respectively. (C-E) Representative TEM images of L2-insulin. The complex was stained by phosphotungstic acid (2%). Complex particles with varied sizes were shown here. Scale bars are 1 μm (C), 0.5 μm (D), and 0.2 μm (E), respectively.

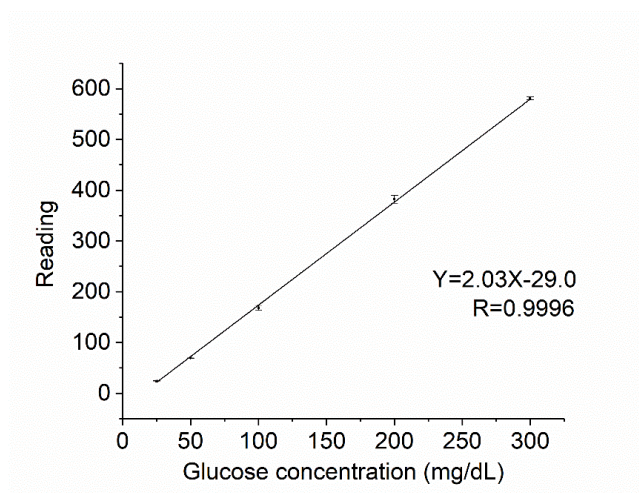


Figure S9. Glucose meter reading as a function of glucose concentration. Data are mean \pm SD ($n=3$).

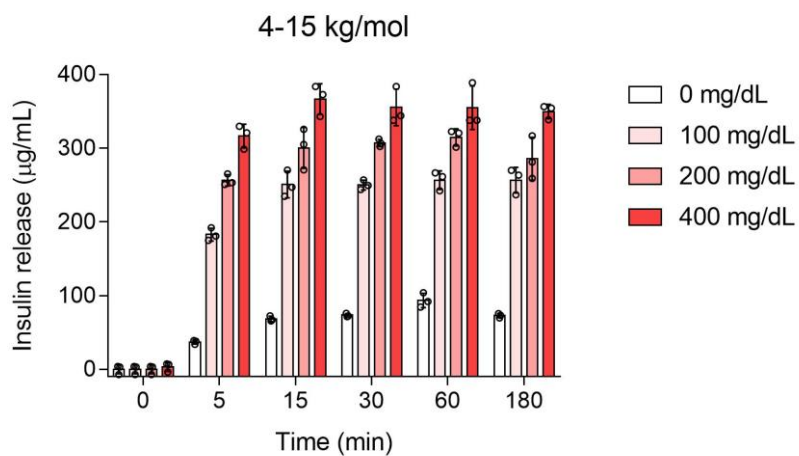


Figure S10. Glucose-responsive insulin release from complex prepared from an equal weight of insulin and PLL_{0.57}-FPBA_{0.43} with the original PLL MW of 4-15 kg/mol. Data are mean \pm SD ($n=3$).

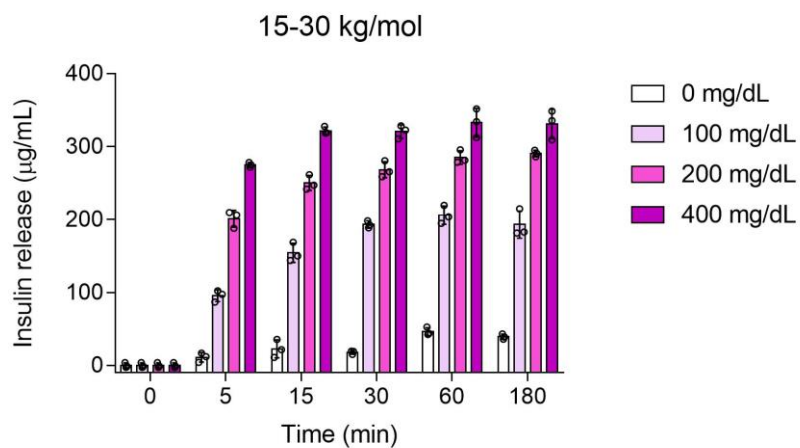


Figure S11. Glucose-responsive insulin release from complex prepared from an equal weight of insulin and PLL_{0.6}-FPBA_{0.4} with the original PLL MW of 15-30 kg/mol. Data are mean \pm SD ($n=3$).

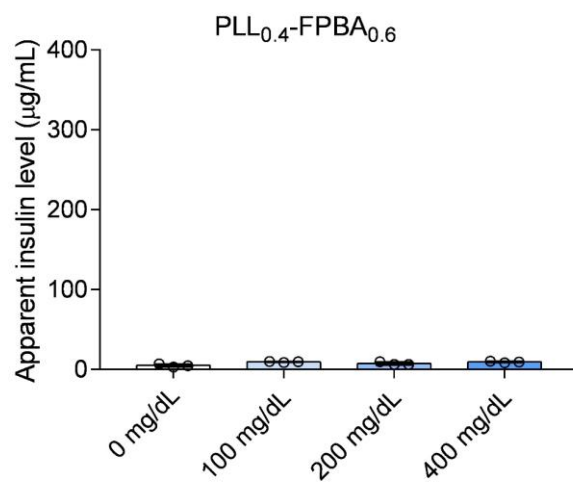


Figure S12. The glucose-dependent solubility of PLL_{0.4}-FPBA_{0.6} in PBS at pH 7.4. The original PLL has a MW of 30-70 kg/mol. The supernatant was centrifuged, collected, and measured using a Coomassie protein assay reagent. The apparent insulin level was calculated according to the standard curve of insulin. Data are mean \pm SD ($n=3$).

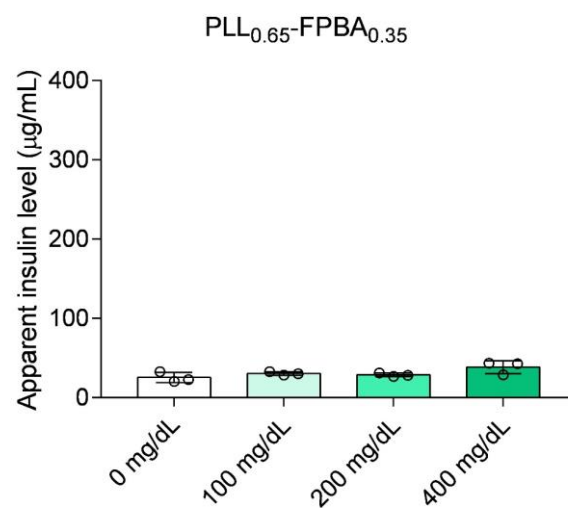


Figure S13. The glucose-dependent solubility of PLL_{0.65}-FPBA_{0.35} in PBS at pH 7.4. The original PLL has a MW of 30-70 kg/mol. The supernatant was centrifuged, collected, and measured using a Coomassie protein assay reagent. The apparent insulin level was calculated according to the standard curve of insulin. Data are mean \pm SD ($n=3$).

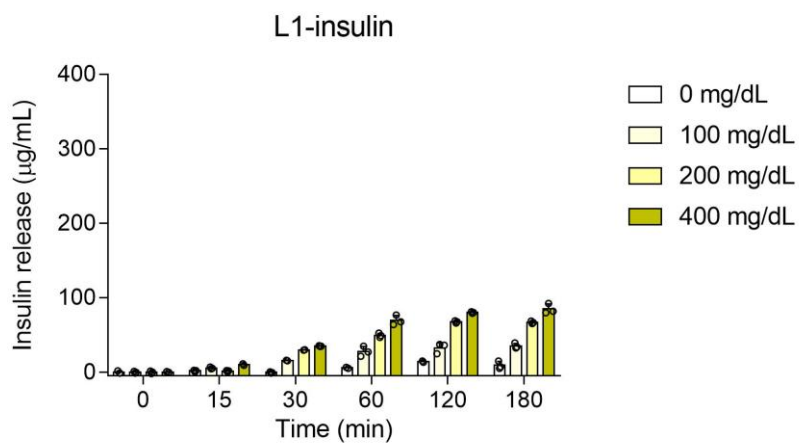


Figure S14. Glucose-dependent insulin release from bulk L1-insulin. L1-insulin was centrifuged (21,000 G, 10 min) to the bottom of Eppendorf tubes. The complex stayed as a bulk at the bottom during the whole experiment. Data are mean \pm SD ($n=3$).

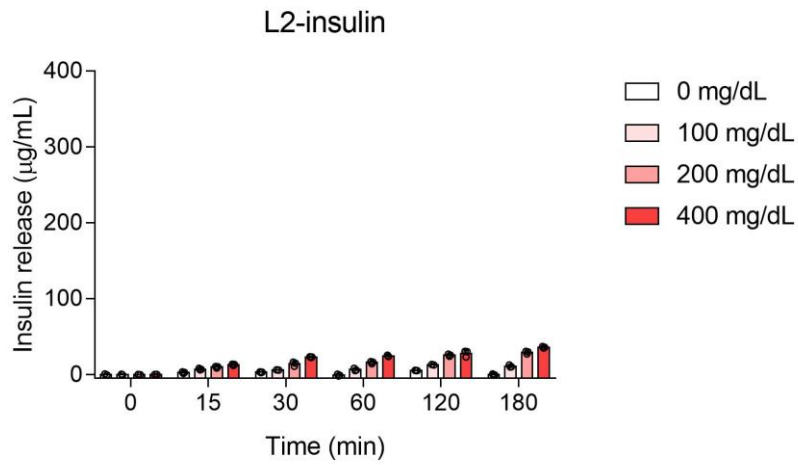


Figure S15. Glucose-dependent insulin release from bulk L2-insulin. L1-insulin was centrifuged (21,000 G, 10 min) to the bottom of Eppendorf tubes. The complex stayed as a bulk at the bottom during the whole experiment. Data are mean \pm SD ($n=3$).

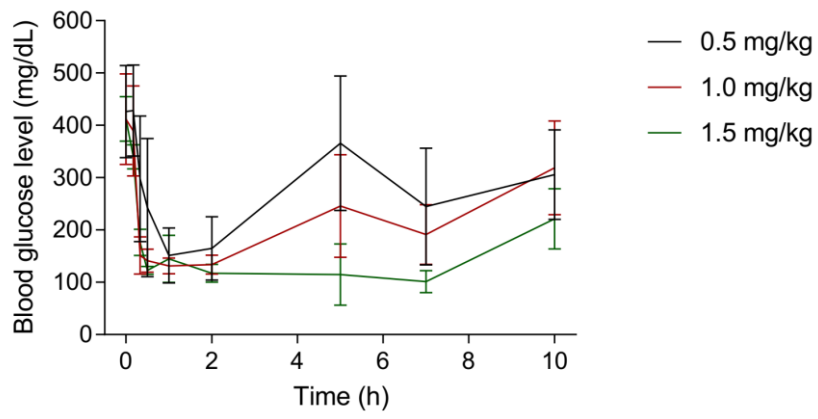


Figure S16. Dose-dependent blood glucose regulation ability of L1-insulin. Data are mean \pm SD ($n=5$).

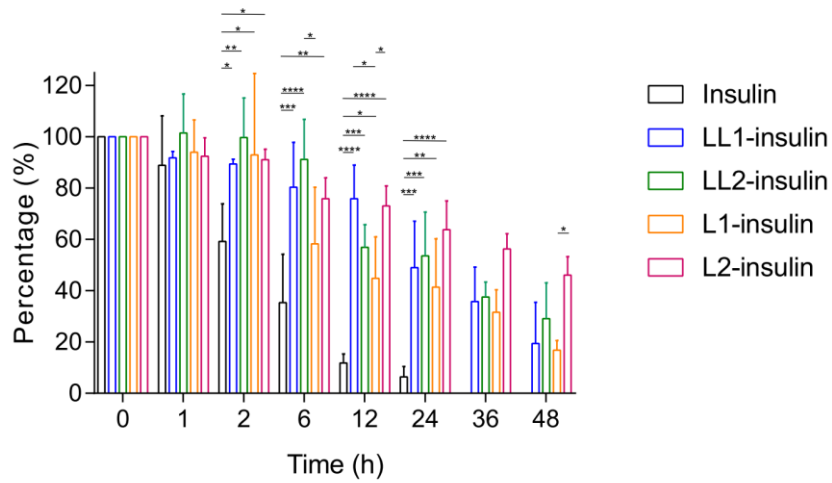


Figure S17. The statistical analysis of fluorescence intensity. Data are mean \pm SD ($n=3$). Two-way ANOVA was used to calculate the difference among difference groups. Only P values with significant difference were shown. $*P < 0.05$, $**P < 0.01$, $***P < 0.001$, $****P < 0.0001$.

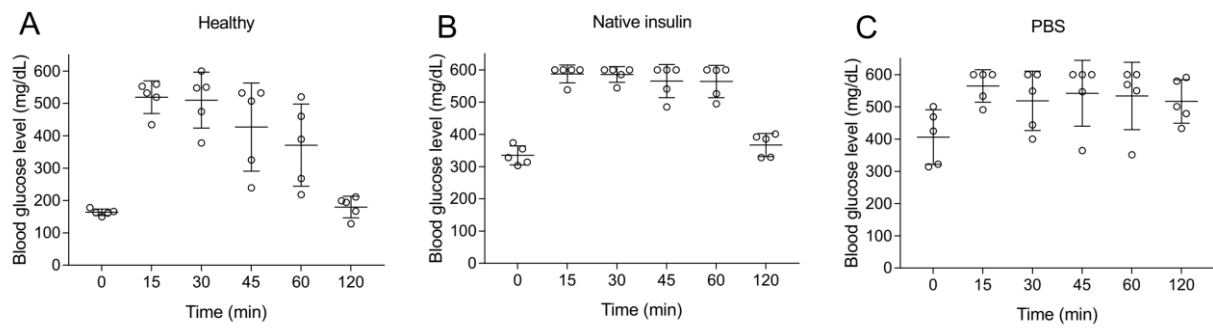


Figure S18. Intra-peritoneal glucose tolerance tests. Healthy mice (A) and diabetic mice receiving native insulin (B) or PBS (C) were used as control groups. The insulin-equivalent dose was set to 1.5 mg/kg. The glucose (3 g/kg) was given at 8 hours posttreatment with complexes. Data are mean \pm SD ($n=5$).

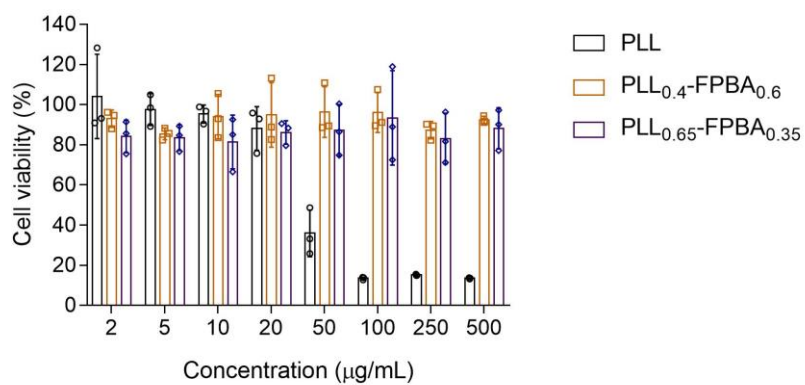


Figure S19. The dose-dependent cytotoxicity of PLL_{30-70k}, PLL_{0.4}-FPBA_{0.6}, and PLL_{0.65}-FPBA_{0.35}. The cytotoxicity was evaluated on L929 murine fibroblast cells. Data are mean \pm SD ($n=3$).

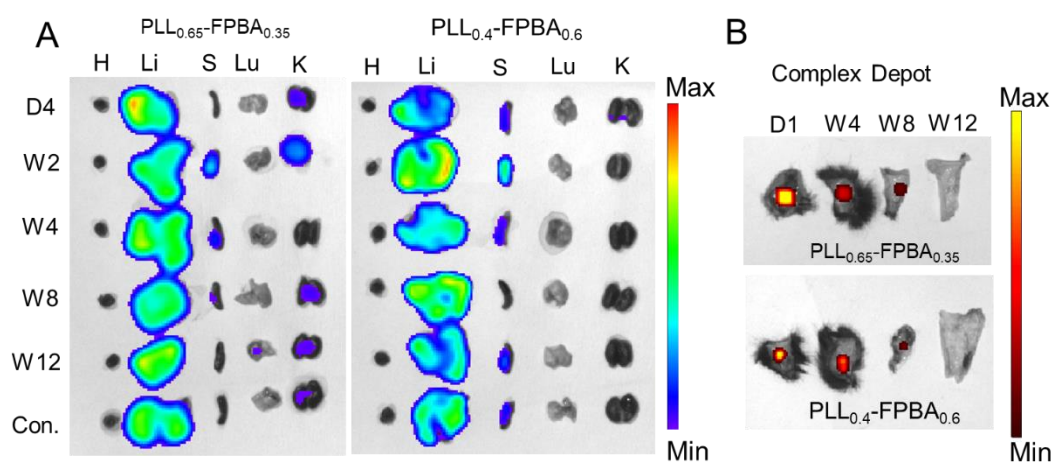


Figure S20. Biodistribution of the polymer after subcutaneous injection. Polymers were labeled with Cy5 and formed complexes LL2-insulin and L2-insulin before injection (1.5 mg/kg insulin-eq. dose). The organs (A) and the skins (B) were obtained between time intervals. IVIS spectrum was used to measure the fluorescence of each organ. H, heart; Li, liver; S, spleen; Lu, lung; K, kidney. Dn, nth day posttreatment; Wn, nth week posttreatment; Con., control group without treatment.

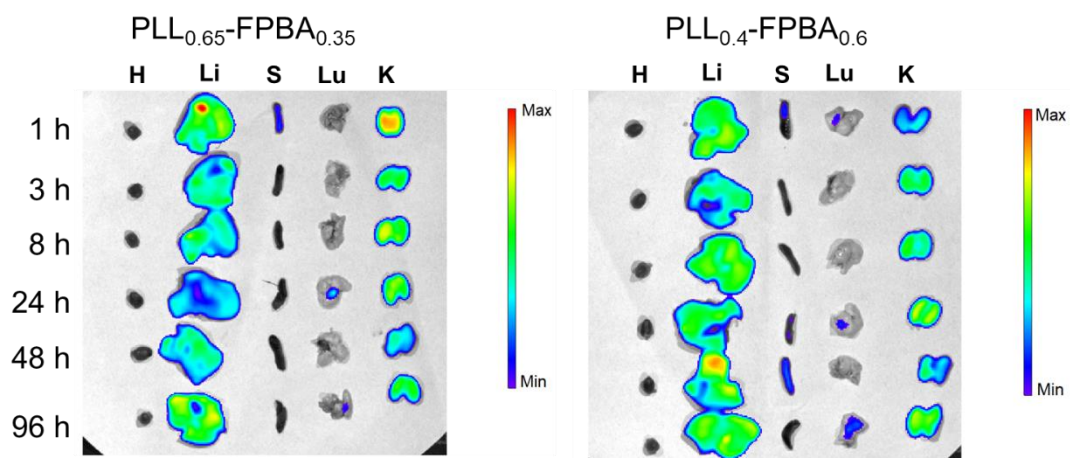


Figure S21. Biodistribution of the polymer after subcutaneous injection. Polymers were labeled with Cy5 and formed LL2-insulin and L2-insulin complexes before injection (1.5 mg/kg insulin eq. dose). The main organs were obtained between time intervals. IVIS spectrum was used to measure the fluorescence of each organ. H, heart; Li, liver; S, spleen; Lu, lung; K, kidney.

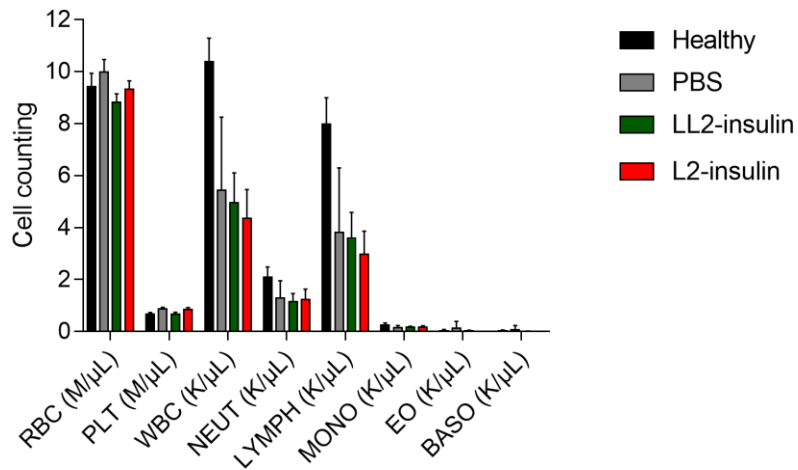


Figure S22. The effect of complex treatment on blood cell count. Diabetic mice were treated with LL2-insulin and L2-insulin every two days at a dose of 1.5 mg/kg. Diabetic mice receiving PBS and healthy mice were used as control groups. Data are mean \pm SD ($n=5$). RBC, red blood cell; PLT, platelet; WBC, white blood cell; NEUT, neutrophil; LYMPH, lymphocyte; MONO, monocyte; EO, eosinophil; BASO, basophil.

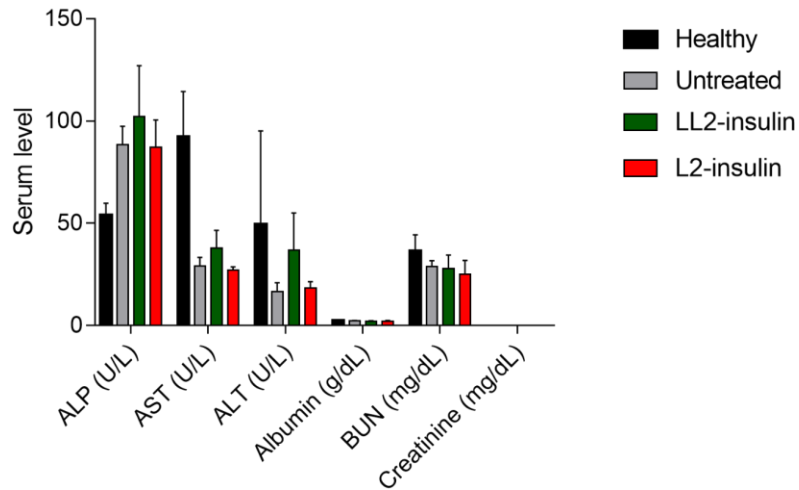


Figure S23. The effect of complex treatment on serum biochemical parameters indicating main organ healthiness. Diabetic mice were treated with LL2-insulin and L2-insulin every two days at a dose of 1.5 mg/kg for one week. Diabetic mice receiving PBS and healthy mice were used as control groups. Data are mean \pm SD ($n=5$). ALP, alkaline phosphatase; AST, aspartate transaminase; ALT, alanine transaminase; BUN, blood urea nitrogen.

Table S1. General features of complexes.

Polymer	Abbreviation	Polymer to-insulin ratio (wt/wt)	N/C ratio (N, amine; C, carboxylic acid)	Z-averaged size (nm)	Zeta-potential (mV) in glucose solution (mg/dL)		
					0	100	400
PLL _{0.65} -	LL1-insulin	1	3.5	4569 ± 632	16.2 ± 4.2	10.0 ± 4.1	6.9 ± 1.0
FPBA _{0.35}	LL2-insulin	2	6.3	2527 ± 1217	20.9 ± 9.1	11.0 ± 2.1	7.2 ± 6.5
PLL _{0.4} -	L1-insulin	1	2.1	3295 ± 1476	-2.5 ± 5.0	-7.0 ± 1.1	-11.9 ± 2.2
FPBA _{0.6}	L2-insulin	2	3.6	2451 ± 1470	-1.6 ± 4.7	-10.0 ± 2.6	-16.1 ± 1.2

Note: Each insulin molecule has six carboxylic acid groups, three amino groups, and one guanidino group, which were all included in the calculation of N/C ratio. Phenylboronic acid groups were not included in the calculation even though they may carry negative charges. Data are presented as mean ± SD ($n=3$).